6-2020

Categorizing zonal productivity on the continental shelf with nutrient-salinity ratios

Jongsun Kim

Piers Chapman

Gilbert Rowe

Steven F. DiMarco

Categorizing zonal productivity on the continental shelf with Nutrient-Salinity ratios

Jongsun Kim [a*] Piers Chapman [a, c], Gilbert Rowe [a, b, c], and Steven F DiMarco [a, c]

[a] Department of Oceanography, Texas A&M University, College Station, TX 77843-3146, USA

[b] Department of Marine Biology, Texas A&M University, Galveston, TX 77553, USA

[c] Geochemical and Environmental Research Group, Texas A&M University, College Station, TX 77843-3149, USA

[*] Corresponding author

*J. Kim. Email: jongsun@tamu.edu

Submit to Journal of Marine Systems

ABSTRACT

Coastal ocean productivity is often dependent on riverine sources of nutrients, yet it can be difficult to determine how far the influence of the river extends. The northern Gulf of Mexico (GOM) receives freshwater and nutrients discharged mainly from the Mississippi and Atchafalaya Rivers. We used nutrient/salinity relationships to (i) differentiate the nutrient inputs of the two rivers and (ii) determine the potential extent of the zones where productivity is affected by each. We identified three different zones: one close to the coast having a linear nutrient/salinity relationship where physical forcing (river flow) dominates, one offshore with nutrient (N or Si) concentrations < 1 μM, and one between them with variable nutrient concentrations largely controlled by consumption by autotrophs. While in the GOM salinity/nutrient relationships varied systematically with distance from the two rivers in winter, this was not seen in summer. Thus, the methodology is not always applicable directly, because the boundaries of the different regions vary with river flow, overall nutrient flux, and grids of stations at the regional spatial scale (15-20 km in the GOM), rather than single sections are needed to determine boundaries.

Keywords:

Coastal productivity; nutrient-salinity relationships; continental shelf

1. Introduction

As is well known, temperature and salinity are useful conservative tracers for identifying different water masses in the ocean (Mamayev, 1975), particularly in the deep ocean where water masses mix along isopycnals. Multi-component mixing has similarly been used frequently to sort out how more than one water mass can mix to match observed concentrations of different parameters (e.g., Tomczak, 1981; Karstensen and Tomczak, 1998; Mohrholz et al., 2008). While temperature/salinity relationships and multi-component analysis can certainly explain physical mixing processes, they cannot explain biological processes (Boyle et al., 1974). In the coastal ocean, however, the water masses are also mixed across isopycnals by tides, winds and currents (Emery and Meincke, 1986; Emery, 2003), and physical-chemical coupling of biological processes is important here and in estuaries (e.g., Harrison et al., 2008; Tang et al., 2015; Wu et al., 2016; Ye et al., 2015).

Nutrient concentrations in estuarine and coastal regions can be either conservative or non-conservative (Liss, 1976; Loder and Reichard, 1981). Conservative mixing leads to a linear correlation between nutrient concentrations and salinity, so that for most components, particularly nutrients, when going from the land to the ocean, there is an inverse relationship with salinity (Johnson et al., 2008; Knee et al., 2010, Wang et al., 2016). The relationship can be positive, however, as shown for iodine in the Yarra estuary, Australia, where both iodate and iodide increased linearly with salinity (Smith and Butler, 1979). Within a river plume, if mixing is conservative, the distance from the land is also related to the concentration of a terrestrial material (Pujo-Pay et al., 2006; Wu et al., 2016). Non-conservative mixing, with a non-linear relationship with salinity, can occur seasonally as a result of biological activity, or from the presence of additional internal sources or sinks in the mixing region. Many studies in coastal waters have used linear regression to predict nutrient and chlorophyll-a concentrations from salinity (e.g., Desmit et al., 2015; Iwata et al., 2005; Hakanson and Eklund 2010). Non-conservative behavior, however, is common. Foster (1973) did not find a linear trend between salinity and UV absorbance off Fiji, while Liss (1976) lists both linear and non-linear trends for the Si/salinity ratio in multiple global rivers.

Most studies of nutrient/salinity relationships have been conducted in estuaries or in the coastal ocean close to an estuary (Desmit et al., 2015; Iwata et al., 2005; Kim et al., 2010; Hakanson and Eklund 2010; Weber et al., 2017; Wu et al., 2016). For instance, Wu et al. (2016) identified additional sources of nutrients that could be differentiated from organic matter decomposition and biological consumption in the Pearl River Estuary. Kim et al., (2010) used nutrients and radon in Korean coastal waters to determine chemical fluxes and to estimate groundwater inputs at the river-ocean interface, while Kim et al. (2011) found that excess nutrients around the volcanic island of Jeju in Korea came from submarine groundwater discharge (SGD). Weber et al., (2017) used nutrient-salinity relationships to determine how nitrogen fixation and export production are influenced by the Amazon River plume. Other authors have discussed conservative/non-conservative mixing using nutrient/salinity plots in regions such as the Amazon River (e.g., DeMaster and Pope 1996; Santos et al., 2008), Pearl River (We et al., 2016), and Changjiang (Yangtze) River (e.g., Gao et al., 2015; Liu et al., 2016; Pei et al., 2009; Wang et al., 2003).

Although the Gulf of Mexico (GOM) is generally oligotrophic, the Texas-Louisiana (LATEX) shelf along its northern edge is greatly affected by heavy nutrient loading from the Mississippi and Atchafalaya Rivers. The two rivers have different nutrient concentrations and their combined nutrient input leads to regular summer hypoxia. Rowe and Chapman (2002), here after called RC02, defined three theoretical zones over the LATEX shelf close to the mouths of these rivers, based on changes in dissolved and suspended parameters. They named these the brown, green, and blue zones. Nearest the river mouths they set the brown zone, where the nutrient concentrations are high, but the discharge of sediment from the river reduces light penetration and limits primary productivity within the river plume. Further away from the river mouth, both offshore and alongshore, they set a green zone with available light and nutrients, and high productivity. In this region, measured nutrient concentrations result from biological uptake processes that vary with the season and river flow (Rabalais et al., 2007; Bianchi et al., 2010). Still further offshore and to the west is the blue zone, dominated by very low surface nutrient concentrations, intense seasonal stratification and a strong pycnocline, so that at this distance from the rivers most primary production is fueled by recycled nutrients (Dortch and Whitledge, 1992). The blue zone merges into oceanic waters offshore, while its inshore edge is defined operationally as the point at which nutrient concentrations decrease below 1 µM. The RC02 model assumes that the edges of the zones (geographical regimes) change over time depending on river flow, biological processes, and productivity, but the model does not attempt to predict such changes.

While RC02 was initially formulated as a way to describe the formation and development of coastal hypoxia, it can also be used to differentiate regions of biological activity from those affected solely by mixing. In this study, we use nutrient/salinity relationships in the coastal waters over the LATEX shelf to define the areas of biological productivity supplied by each river. We then compare our results with those of Lahiry (2007), who defined the edges of the RCO2 brown and green zones solely from salinity changes. While Kim et al. (2020) have examined the RC02 hypothesis with a box model, here we use the three zone hypothesis to differentiate explicitly the relationships between *in situ* nutrient data and different river sources (Kim et al. 2020). This allows us to show not only how multiple source waters mix, but also how far from the source their biological influence extends. These two effects need not be the same, especially when nutrients are being discharged into relatively oligotrophic coastal oceans, where biological activity can reduce their concentration long before the physical presence of low salinity water disappears.

2. Data and Methods

2.1. Study area and Data

2.1.1. The Gulf of Mexico (GOM)

Hydrographic data (T, S, O and nutrients) from three projects - LATEX (The Louisiana-Texas Shelf Physical Oceanography Program), MCH (Mechanisms Controlling Hypoxia), and NEGOM (North Eastern Gulf of Mexico), as well as monthly data from LUMCON (Louisiana Universities Marine Consortium) were collected from the National Oceanographic Data Center (https://www.nodc.noaa.gov). The data covered the period from 1991 through 2014 (Table 1, Fig. 1). Quality control (e.g. removing outliers, missing data interpolation) removed inconsistencies and data anomalies. Parameters examined were temperature (T), salinity (S), and dissolved nitrate, phosphate and silicate (DIN, DIP, and DSi), although DIP is not used in this paper as it is known to be affected by desorption from particles during estuarine-ocean mixing (Liss, 1976; DeMaster and Pope, 1996). The data were first separated into summer (May ~ July) and winter (November ~ March) periods to look at seasonal variability. Second, all nutrient data sets were plotted against salinity to see if there were any consistent relationships; this was also done year-by-year and cruise-by-cruise. LUMCON data were the only data collected seasonally on a consistent basis, and there were relatively few winter cruises (Table 1). C-line data were collected approximately monthly, while the F line was sampled less frequently. Because the region is highly stratified in summer, we considered only data taken from above the pycnocline.

2.1.2. End-member determination

To determine nutrient concentrations in the GOM freshwater end-members, data were obtained from United State Geological Survey (USGS) for stations at Baton Rouge (USGS station number 07374000) on the Mississippi River and Morgan City (USGS station number 07381600) on the Atchafalaya River. We defined the spring period as March to May, summer as June to August, fall as September to October, and winter as November to March, based on known variability in wind, currents and river discharge. The concentration of nitrate + nitrite (NO_{3+2}) at Baton Rouge from 1992 through October 2016 varied between 50 ~ 200 μM, being generally lower in winter than in spring. Monthly means of daily NO_3+NO_2 data from February 18th, 2015 through October 22nd, 2016 are given in Figure 2; before this period daily data from both rivers were not available, as collection of nitrate data from Morgan City on the Atchafalaya only started in December 2014. Dissolved N concentrations and fluxes typically increase from March to June in both years because of snow melt and rainfall in the upper catchment of the Mississippi-Atchafalaya River System (MARS). The Atchafalaya River contains water both from the Red River and from the Mississippi. Concentrations in the Red River are lower than in the Mississippi, which accounts for the difference seen in Figure 2b.

We made the initial assumption that in all regions changes in DIN and DSi concentrations between the freshwater end-member and coastal seawater were conservative, with concentrations decreasing consistently as salinity increases. Details of DIN end-member range, standard deviation, median, and mean are in Table 2. These are compared with monthly data from the same two sites reported by USGS for the period 2000 ~ 2018.

2.2. Method: Correlations between terrestrial components and salinity ratio

We identified the different regions defined by RC02 using winter data initially. Winter nutrient concentrations are considerably higher and likely more conservative than in summer, when high phytoplankton production rapidly reduces nutrients to low levels, making it hard to see any relationship. While RC02 may hold in summer, because of reduced river flow the brown zone will be much closer inshore where there was no sampling.

In conservative mixing, the nutrient concentration along the salinity gradient varies linearly as described by equation 1 (Boyle et al., 1974; Kim, 2018).

$$\boldsymbol{N_C} = \boldsymbol{m} * \boldsymbol{S} + \boldsymbol{N_0} \quad \text{....(1)}$$

where $\boldsymbol{N_c}$ is the concentration of nutrients including DIN and DSi, **m** is a slope, $\boldsymbol{S}$ is salinity, and $\boldsymbol{N_0}$ represents the nutrient intercept at S = 0, respectively. $\boldsymbol{N_0}$ can be compared directly to the end-member data.

The important concepts of the RC02 model are: (I) coastal zone nutrient concentrations in the euphotic layer are fully supported by river input because the surface seawater concentration in the offshore GOM is low; (II) nutrient concentrations decrease from the brown zone to the green zone because of uptake by phytoplankton and/or dilution with offshore water; (III) nutrient concentrations in the blue zone are always low and assumed to be <1 μM for nitrate so that biological productivity is also low; (IV) there is no physical boundary between the zones because the water is continuously moving; and (V) the edges of the three zones vary with time depending on freshwater flow and nutrient concentration. The model therefore describes a continuum of nutrient concentrations with variable internal boundaries. While keeping the basic RC02 hypothesis, we modified their theoretical model, using historical nutrient data from the GOM region, as shown in Figure 3.

When freshwater with high nutrient concentrations and seawater with low concentrations are mixed together, conservative mixing will produce a linear mixing relationship between the freshwater end member and the outer edge of the green zone at a typical salinity for the coastal GOM of ~33 (red dotted line in Figure 3). We assume that dilution is more important than biological uptake in the brown zone, although some uptake will still occur, so that the blue shaded triangle indicates theoretical removal through biological production in both brown and green zones (Figure 3). Thus, the area within the triangle indicates the total quantity of nutrients taken up by phytoplankton in the coastal zone. Note that Figure 3 makes no allowance for the actual area covered by each zone and the green zone is in practice considerably larger than the brown zone in the northern GOM. The boundary between the brown and green zones is the point at which the observed slope of the nutrient/salinity plot changes in the mid-salinity region of the graph, and the green zone extends offshore until the DIN concentration falls below 1 μM. This will vary from cruise to cruise based on river flow, nutrient concentration, and phytoplankton activity.

This conceptual diagram based on the RC02 three zone model as it applies to one river (Figure 3). A similar diagram can be drawn for the other river. We did not attempt to quantify the interaction between the two freshwater sources, merely to determine how far the influence of each extends. While two brown zones will show clearly how far the main plumes of each river extend, if the two green zones overlap, one can perhaps determine the relative contributions of each source from multi-parameter relationships (Tomczak, 1981). In the northern GOM, non-summer flow is typically from east to west (Cochrane and Kelly, 1986), so it is likely that the green zone between the Atchafalaya and Mississippi Rivers is derived largely from the Mississippi, and that west of about 92°W the green zone derives mainly from the Atchafalaya.

3. Results

3.1. Nutrient/salinity relationships as tracers for water masses

3.1.1. MCH data (M4 cruise; March 2005)

Almost all MCH cruises took place during the spring and summer period because they were investigating the development of hypoxia on the Louisiana shelf. Plotting summer data from these cruises (not shown) showed no obvious differences initially between regions of the shelf closest to the Mississippi and Atchafalaya, mainly because the nutrient concentrations above the pycnocline were too low, while below it they both sampled essentially the same water mass, derived from high salinity offshore water.

Data from the only winter cruise in March, 2005, however, illustrated the distinct difference above the pycnocline between the two different water sources (Figure 4) for both DIN and DSi. There was a strong linear relationship at salinities < 22 near the Atchafalaya for both DIN and DSi and below a salinity of about 28 in the region near the Mississippi. Near the Atchafalaya, the DIN and DSi concentrations remained fairly constant at salinities between 28 and 33, dropping to 1 μM or less further offshore as the salinity increased. Off the Mississippi, however, DIN concentrations continued to decrease across the green zone, while DSi concentrations were more variable, possibly because of the proximity of the delta and local circulation patterns. Below the pycnocline, all data fell on the same line at salinities > 33 (not shown).

From USGS data the range of the annual freshwater end-members in both rivers is about 70 µM ~ 100 µM for DIN and 80 µM ~ 120 µM for DSi (Fig. 2, Table 2, Putnam-Duhon et al., 2015). Observational data from the MCH M4 cruise gave the DIN concentrations for end-members (i.e., estimated N-intercept of nutrients) of 64.88 µM for the Atchafalaya River and 73.65 µM for the Mississippi River, respectively at this time. This compares with USGS data from Morgan City and Baton Rouge during March 2005 of 70.0 and 119.3 µM respectively. DSi end-member concentrations were estimated similarly as 86.96 µM for the Atchafalaya River and 104.61 µM for the Mississippi River (USGS data do not include dissolved silicate at this time). Thus, the intercepts produced from nutrient/salinity relationship plots from this cruise fell within the envelope estimated from the USGS data for Si and only slightly below it for DIN. These intercepts refer only to this cruise; intercepts at other times differ depending on water flow and nutrient concentrations.

The salinity-nutrient (DIN and DSi) relationships above the pycnocline for the different water sources during this cruise had different gradients. For DIN, both slopes were similar and significant ($P < 0.0001$) with $R^2 = 0.8078$ for the Mississippi river region and 0.7798 for the Atchafalaya river region, respectively. At salinities > 33, there was no difference between the two regions because both regions contained mainly offshore water. However, the DSi/salinity slope near the Mississippi was less than that near the Atchafalaya, and the correlation was also less, with $R^2 = 0.5512$ for the Mississippi region and 0.9721 for the Atchafalaya region ($P < 0.0001$ in both regions). Off the Atchafalaya, the DIN (NO_{3+2}) and DSi concentrations were approximately constant at higher salinity (around 25) until the salinity reached 33. Based on the data from this one cruise, we can apparently use winter nutrient and salinity relationships as tracers to delineate the boundaries for mixing from the two major river plumes in this region.

3.1.2. LATEX data (H04 cruise; February 1993)

The LATEX H04 cruise (February 1993) provided the only winter data from the LATEX project. Station locations are shown in Figure 1, and the nutrient/salinity plots (Figure 5) followed a similar pattern to the MCH M4 data in Figure 4. It should be noted that the sampling locations from the MCH and LATEX cruises were different, and that LATEX data were only sampled along one transect, while MCH data were sampled over a larger region (Figure 1). Thus, the smaller LATEX data set is unlikely to give as good a result as the more extensive MCH 4 data. Early 1993 was very wet relative to the long-term mean (RC02), so this may have overwhelmed the contribution from the Red River, which provides much of the flow in the Atchafalaya, as the nutrient/salinity relationships for both lines were very similar. However, while the boundary between the green and blue zones was again found at S =33, the brown/green transition was at about S= 30 for the Atchafalaya region and between 31-34 for the Mississippi. Based on the data the predicted DIN end-member from the Atchafalaya River was 35.95 µM and that for the Mississippi River was 47.93 µM, while predicted DSi end-members were 82.86 µM for the Atchafalaya River and 82.33 µM from the Mississippi River respectively, but there were no USGS data during this period.

The DIN and DSi relationships for the two river sources had different slopes during this LATEX H04 cruise from those found during MCH 4. For DIN, both slopes are similar and highly significant ($P < 0.0001$) with $R^2 = 0.8553$ for the Mississippi river region and 0.8624 for the Atchafalaya river region, respectively. As for the MCH M4 data, there was no difference at salinities over 33 in the offshore water, either above or below the pycnocline. The DSi/salinity slopes near both regions were also highly significant ($P < 0.0001$) and similar, with R^2 being 0.9620 for the Mississippi region and 0.8892 for the Atchafalaya region.

3.1.3. LUMCON data (C & F transects above/below pycnocline layers)

Similar to LATEX data, but unlike the MCH M4 data, the sampling stations for LUMCON data (Figure 1) were along only one transect near each river. LUMCON cruises took samples each month, starting in 1985, but not all months were sampled in all years and the F line off the Atchafalaya was sampled less frequently than the C line. In this study, we used only winter data from 2001 through 2010 (Table 3). Similar to the MCH and LATEX data, the LUMCON data from below the pycnocline all had $S > 33$ and fell on the same relationship during each cruise, even though the C and F regions had different pycnocline layer depths (approximately 10m and 15m for the C and F regions respectively), as determined by density changes coinciding generally with at least a 0.5 ml/L change in oxygen concentration, and there were no apparent nutrient/salinity relationships.

Because the general flow along the coast in winter is from east to west, we assumed initially that C line data originated from the Mississippi and F line data from the Atchafalaya River. Taking all the data from above the pycnocline on all LUMCON winter cruises, samples from the F line showed stronger nutrient/salinity relationships than C line data across the whole salinity range for both DIN and DSi (Figure 6). For the F line data, the R^2 values were 0.6011 for DIN and 0.7851 for DSi, with $P < 0.0001$ for both. R^2 values were much lower along the C line at 0.1471 for DIN and 0.3658 for DSi. Summer R^2 values (not shown), were all less than 0.075. The results varied probably both because the sampling stations along the C line were further from the Mississippi River mouth than the F transect was from the Atchafalaya and because we used all the available winter data from this period. When individual cruises were considered, however, better correlations appeared (Figure 7), but this was not always the case (Table 3), and most of the relationships along the C and F lines predicted low values for the end members, in the 40-60 μM range, e.g., during March 2009 (Figure 7). The low slopes of the nutrient/salinity relationships and the relatively invariant salinities (all the salinities along the C lines are > 25) suggested that all the data were taken in the green zone.

3.1.4. Quantification of RC02 model from historical data

Based on the relationships shown above, we can set the nutrient and salinity concentrations at the zonal boundaries from these cruises, including summer cruises. Based on the MCH data, the salinity and nutrient ranges of each zone in GOM are: brown zone - salinity < 25, for DIN 5 ~ 75 μM; green zone - salinity between 25 ~ 32, DIN 1 ~ 5 μM; and blue zone - salinity > 32, DIN 0 ~ 1 μM, respectively. The boundaries were identified similarly using LATEX and LUMCON data, however, it was harder to define the portions of the nutrient boundary between the green and blue zones, because of fewer data points and the distance of the C line and the 90°W LATEX line from the Mississippi River mouth.

The boundaries of the three zones for each cruise are shown in Figure 8. While the brown zone could be seen in all cruises near the Mississippi, it was absent in both M3 and M5 cruises near the Atchafalaya River). It seems that the river water was rapidly mixed during discharge within Atchafalaya Bay. In addition, from these results we can initially see where the water masses flow and mix. For instance, according to MCH M4 and M5 cruise data, the boundary of the green zone can extend from near the delta as far as 91°W between the Mississippi and Atchafalaya rivers, and even further on occasion. However, the brown zones are restricted to small regions near the river mouths.

4. Discussion and conclusions

Our study has used nutrient/salinity relationships to identify the water sources in the coastal GOM, and explain how well the RC02 hypothesis of three zones can be used to identify regions of biological importance in the presence of two competing nutrient sources and differentiate between them. Lahiry (2007) used salinity with the RC02 hypothesis to define the edges of the zones in the coastal GOM and thus regions where hypoxia could be expected. Replotting these data (Figure 9) indicated patterns similar to ours for cruises MCH M1-M3, especially near the Mississippi delta, where conservative mixing was expected. Thus, either using salinity alone or a combination of nutrients and salinity, similar boundaries could be identified in this region. Near the Atchafalaya River and between the Mississippi and the Atchafalaya rivers, however, we found very different boundaries for the three zones (compare Figures 8 and 9). While salinity can define how far the river water plume extends and mixes with oceanic water, the nutrient and salinity relationships can incorporate more complex biological processes when two different water masses mix. Thus, we can determine the region affected by the river in terms of productivity. Using nutrient and salinity relationships to differentiate different productivity zones enhances our interpretations of biological processes in the GOM. While Lahiry (2007) concluded that the three zones may be more significantly applicable to smaller spatial scales (< 10 Km), the spatial scale of the Texas-Louisiana shelf is about 15 to 20 Km both alongshore and offshore (Li et al., 1996).

Our results can be compared to similar work from several other large rivers in Table 4, based on our interpretation of nutrient/salinity plots in these publications. Where nitrate and silicate showed different boundaries, these are shown separately. Phosphate data are not included because several authors report phosphate desorption from particulate matter at salinities between 15-25 (e.g., DeMaster and Pope, 1996; Santos et al., 2008 for the Amazon; van Bennekom et al., 1978 for the Zaire River). Where no values are given for the position of the brown-green zonal boundary, the data showed conservative mixing throughout the sampling regime, as was found in winter cruise. This was found in winter cruises off the Changjiang by Edmond et al. (1985) and Gao et al. (2015). Somewhat surprisingly, given that the region offshore of the Changjiang is generally well stratified in summer, during the flood season (Gao et al., 2015; Liu et al., 2016), fully conservative mixing was found also in July 2001 by Zhang et al. (2007). Green-blue zonal boundaries assume nutrient levels were close to zero.

As can be seen from Table 4, all rivers shown here exhibited an initial loss of nutrients, compared with concentrations expected from conservative mixing, at salinities generally between 10 and 25, particularly when the offshore region is stratified. We assume that this can be considered the outer edge of our brown zone. In many cases, including all studies cited off the Changjiang and the DeMaster and Pope (1996) observations off the Amazon, this coincided with a decrease in turbidity and suspended sediment, and often also with a salinity front (e.g., Shen, 1993; Liu et al. 2016). Similar observations are found in the northern GOM; continuous data from Acrobat tows across the Louisiana shelf during multiple cruises in summer show excellent correlations between low salinity and high turbidity and colored dissolved organic matter (CDOM) close to the river mouths (DiMarco and Zimmerle, 2017). DeMaster and Pope (1996) also reported an increase in primary productivity offshore of this boundary. This agrees with the idea in RC02 that light limitation sets the outer boundary of the brown zone. Variations on river flow affect both the salinity and distance offshore at which the boundary is found. Using the DeMaster and

Pope (1996) Amazon data as examples, the salinity at the boundary varied between 10 (high discharge, March, May 1990) and 20 (falling discharge, August 1989). During low discharge conditions, in November 1991, initial decreases occurred at a salinity of about 13-15. Similar results were reported for nitrate by Santos et al. (2008), but not by Weber et al. (2017), although in the latter case all samples were taken well away from the river mouth to the north west and the minimum salinity found was only 16.6. As a result, all the nitrate had been taken up by phytoplankton and concentrations were almost all below 0.1 μM/L, but silica concentrations only began to decline at about S=18. It seems likely that in this particular case, samples were taken towards the outer edge of the green zone, or even in the blue zone.

Additional data supporting the RC02 three zone hypothesis are also common from the Changjiang, especially during the summer flood season when stratification is the normal condition and nutrient concentrations are highest (Edmond et al., 1985; Shen, 1993; Tian et al., 1993; Zhang et al., 2006; Gao et al., 2015; Liu et al. 2016). Nutrient concentrations in offshore water (the blue zone) in the East China Sea approach zero at salinities above 28 in summer (Table 4), so the green zone is narrow here in salinity space although quite wide in area. Again, this is similar to the data from the Louisiana shelf.

The idea of three zones exists also in rivers with lower suspended sediment concentrations than the Amazon, as shown by data from the Para River in November 1991 (DeMaster and Pope, 1996) and also in the Zaire (van Bennekom etal. 1978). In the former, nitrate and silicate declined rapidly at low salinities, presumably because of the lower sediment loads, but silicate (and phosphate) increased offshore at salinities above 30, where nitrate concentrations were close to zero. The Zaire, however, did not show a nutrient decrease until higher salinities (~25), possibly because of high dissolved organic matter concentrations that can also cause light limitation (van

Bennekom et al., 1978) or short residence time for shelf water that leads to low phytoplankton populations (Cadee, 1978).

To sum up, we have confirmed that nutrient/salinity plots can be used to identify different regions of biological productivity during river mixing into the coastal ocean, but not always in all seasons. In the GOM, inputs from the two rivers can clearly be differentiated in winter, but during summer, the rapid biological uptake makes it hard to see the pattern in the nutrient/salinity ratios. Because summer is the low flow regime for rivers in the northern GOM (Figure 2), the brown zone presumably occurs much closer to the estuaries of the Mississippi and Atchafalaya than we were able to sample. If one can assume, however, that the salinity boundaries identified in winter nutrient/salinity plots are generally consistent from one season to another, they can be applied to data collected at other times of the year. Clearly, the method only works where there is an obvious source of nutrients, and the further from the source one samples, the harder it is to determine what zone you are in or, in areas with more than one source, which one supplies the nutrients to a particular region. For this reason, a grid of stations provides considerably more information than single sections, especially at small scales when the brown zone is close to the river mouth.

Traditionally, temperature/salinity data can provide useful information on mixing within the coastal ocean, but they can only explain physical processes (Boyle et al., 1974). Because the water is always moving, the edges of the zones are constantly changing, and sampling needs to consider the physical scales of the region being studied. However, the results from this work suggest that for systems with large inputs at least, it is possible to use simple relationships, such as DIN or DSi with salinity, to determine how far the influence of each source on local productivity extends. Based on a comparison of our data with previous studies in other large river systems, it appears that our brown/green boundary can often be aligned with either salinity or turbidity fronts and that our approach can be useful to identifying productivity boundaries in the coastal ocean.

Acknowledgements

The authors would like to thank to the captain and crew of the R/V Gyre, R/V Pelican, and R/V Manta along with the many marine technicians and students who participated in the cruises. This research was made possible by grant SA 12-09/GoMRI-006 to the Gulf Integrated Spill Consortium from the Gulf of Mexico Research Initiative and by grants NA03NOS4780039, NA06NOS4780198, and NA09NOS4780208 from NOAA. Hydrographic and dissolved nutrients data used in this study from the Texas-Louisiana Shelf from years 2004-2009 are available from NOAA NCEI (accession-ID 0088164). We also thank the anonymous reviewer for suggestions that improved the manuscript.

References

Bianchi, T.S., DiMarco, S.F., Cowan Jr., J.H., Hetland, R.D., Chapman, P., Day, J.W., Allison, M.A., 2010. The Science of hypoxia in the Northern Gulf of Mexico: A review. Science of the total Environment 408(7), 1471-1484.

Boyle, E., Collier, R., Dengler, A.T., Edmond, J.M., NG, A.C., Stallard, R.F., 1974. On the chemical mass-balance in estuaries. Geochimica et Cosmochimica Acta 38, 1719-1728.

Cadee. G.C. 1978. Primary production and chlorophyll in the Zaire River, estuary and plume. Netherlands Journal of Sea Research, 12, 366-381.

Cochrane, J.D., Kelly, F.J., 1986. Low-frequency circulation on the Texas-Louisiana continental shelf. Journal of Geophysical Research. 91(C9), 10645-10659.

DeMaster, D.J., Pope, R.H., 1996. Nutrient dynamics in Amazon shelf waters: results from AMASSEDS. Continental Shelf Research. 16. 263-289.

Desmit, X., Ruddick, K., Lacroix, G., 2015. Salinity predicts the distribution of chlorophyll a spring peak in the southern North Sea continental waters. Journal of Sea Research 103, 59-74.

DiMarco, S.F., Zimmerle, H.M. 2017. MCH Atlas: Oceanographic Observations of the Mechanisms Controlling Hypoxia Project. Texas A&M University, Texas Sea Grant, Publication TAMU-SG-17-601, 300 pp.

Dortch, Q., Whitledge, T.E., 1992. Does nitrogen or silicon limit phytoplankton in the Mississippi River plume and nearby regions? Continental Shelf Research 12, 1293-1309.

Edmond, J.M., Spivack, A., Grant, B.C., Hu, M-H., Chen, Z., Chen, S., Zeng,X., 1985. Chemical dynamics of the Changjiang estuary. Continental Shelf research 4, 17-36.

Emery, W.J., Meincke, J., 1986. Global water masses: summary and review. Oceanologica Acta. 9, 383-391.

Emery, W.J., 2003. Water types and water masses. Ocean Circulation/Water Types and Water Masses. pp. 1556-1567.

Forsberg, B.R., Devol, A.H., Richey, J.E., Martinelli, L.A., Santos, H.D., 1988. Factors controlling nutrient concentrations in Amazon floodplain lakes. Limnology and Oceanography. 33 (1) 41-56.

Foster, P., 1973. Ultraviolet absorption/salinity correlation as an index of pollution in inshore sea waters. New Zealand Journal of Marine and Freshwater Research 7(4), 369-379.

Gao, L., Li, D., Ishizaka, J., Zhang, Y., Zong, H., Guo, L., 2015. Nutrient dynamics across the river-sea interface in the Changjiang (Yangtze River) estuary–East China Sea region. Limnology and Oceanography. 60. 2207-2221.

Hakanson, L., Eklund, J.M., 2010. Relationships between chlorophyll, salinity, phosphorus, and nitrogen in lakes and marine areas. Journal of Coastal Research 26, 412-423.

Harrison, P.J., Yin, K.D., Lee, J.H.W., Gan, J.P., Liu, H.B., 2008. Physical–biological coupling in the Pearl River Estuary. Continental Shelf Research 28, 1405–1415. https://doi: org/10.1016/j.csr.2007.02.011.

Iwata, T., Shinomura, Y., Natori, Y., Igarashi, Y., Sohrin, R., Suzuki, Y., 2005. Relationship between salinity and nutrients in the sub-surface layer in the Suruga Bay. Journal of Oceanography 61, 721-732.

Johnson, A.G., Glenn, C.R., Burnett, W.C., Peterson, R.N., Lucey, P.G., 2008. Aerial infrared imaging reveals large nutrient-rich groundwater inputs to the ocean. Geophysical Research Letters 35(15), L15606.

Karstensen, J. Tomczak, M., 1998. Age determination of mixed water masses using CFC and oxygen data. Journal of Geophysical Research 103, 18599-18609.

Knee, K.L., Street, J.H., Paytan, A., Grossman, E.E., Boehm, A.B., 2010. Nutrient inputs to the coastal ocean from submarine groundwater discharge a groundwater-dominated system: Relation to land use (Kona coast, Hawaii, U.S.A.). Limnology and Oceanography 53(3), 1105-1122.

Kim, G., Kim, J.S., Hwang, D.W., 2011. Submarine groundwater discharge from oceanic islands standing in oligotrophic oceans: Implications for global production and organic carbon fluxes. Limnology and Oceanography 56(2), 673-682.

Kim, J.S., Lee, M.J., Kim, J., Kim, G., 2010. Measurement of Temporal and Horizontal Variations in ^{222}Rn Activity in Estuarine Waters for Tracing Groundwater Inputs. Ocean Science Journal. 45(4), 197-202.

Kim, J.S., 2018. Implications of different nitrogen input sources for primary production and carbon flux estimates in coastal waters. Texas A&M University. Ph.D. Dissertation.

Kim, J.S., Chapman, P., Rowe, G., DiMarco, S. F., Thornton, D.C.O:, 2020. Implications of different nitrogen input sources for potential production and carbon flux estimates in the coastal Gulf of Mexico (GOM) and Korean coastal waters. Ocean Science. 16, 45–63..

Lahiry, S., 2007. Relationships between nutrients and dissolved oxygen concentrations on the Texas-Louisiana shelf during spring-summer of 2004. Texas A & M University. MS. Thesis.

Li, Y., Nowlin, W.D., Reid, R.O., 1996. Mean hydrographic fields and their inter-annual variability over the Texas-Louisiana continental shelf in spring summer and fall. Journal of Geophysics Research 102, 1027-1049.

Liss, P.S., 1976. Conservative and non-conservative behaviour of dissolved constituents during estuarine mixing, in: Burton, J.D., Liss, P.S. (Eds.), Estuarine chemistry. Academic Press, London, pp. 93-130.

Liu, S.M., Qi, X.H., Li, X., Ye, H.R., We, Y., R, J.L., Zhang, J., Xu, W.Y., 2016. Nutrient dynamics from the Changjiang (Yangtze River) estuary to the East China Sea. Journal of Marine Systems. 154. 15-27.

Loder, T.C., Reichard, R,P., 1981. The Dynamics of Conservative Mixing in Estuaries. Estuaries 4 (1), 64-69.

Mamayev, O.I., 1975. Temperature-Salinity analysis of world ocean waters, Elsevier Oceanography Series #11. Elsevier Scientific Pub. Co., Amsterdam.

Mohrholz, V., Bartholomae, C.H., van der Plas, A.K., Lass, H.U., 2008. The seasonal variability of the northern Benguela undercurrentand its relation to the oxygen budget on the shelf. Continental Shelf research 28, 424-441.

Pei, S., Shen, Z., Laws, E., 2009. Nutrient dynamics in the upwelling area of Changjiang (Yangtze River) Estuary. Journal of Coastal Research. 25 (3). 569-580.

Pujo-Pay, M., Conan, P., Joux, F., Oriol, L., Naudin, J.J., Cauwet, G., 2006. Impact of phytoplankton and bacterial production on nutrient and DOM uptake in the Rhone River plume (NW Mediterranean). Marine Ecology Progress Series 315, 43-54.

Putnam-Duhon, L., Hay, A., Latuso, K., Sheehan, J., Vincent, A., 2015. Louisiana Department of Environmental Quality (LDEQ). 2015. Nitrogen and Phosphorus Trends of Long-Term Ambient Water Quality Monitoring Sites in Louisiana. Office of Environmental Services, Louisiana Department of Environmental Quality, Baton Rouge, LA.

Rabalais, N.N., Turner, R.E., Sen Gupta, B.K., Boesch, D.F., Chapman, P., Murrell, M.C., 2007. Hypoxia in the northern Gulf of Mexico: Does the science support the plan to reduce, mitigate, and control hypoxia? Estuaries Coastal. 30, 753-772.

Rowe, G.T., Chapman, P., 2002. Continental Shelf Hypoxia: some nagging questions. Gulf Mexico Science. 20, 153-160.

Santos, M.L.S., Muniz, K., Barros-Neto, B., Araujo, M., 2008. Nutrient and phytoplankton biomass in the Amazon River shelf waters. Annals of the Brazilian Academy of Sciences. 80 (4), 703-717.

Shen, Z., 1993. A study on the relationships of the nutrients near the Changjiang River estuary with the flow of the Changjiang River water. Chinese Journal of Oceanology and Limnology. 11, 260-267.

Smith, J.D., Butler, E.C.V., 1979. Speciation of dissolved iodine in estuarine waters. Nature, 277, 468-469.

Tang, C.H., Wong, C.K., Lie, A.A.Y., Yung, Y.K., 2015. Size structure and pigment composition of phytoplankton communities in different hydrographic zones in Hong Kong's coastal seas. Journal of the Marine Biological Association of the United Kingdom 95, 885–896. https://doi: 10.1017/s0025315415000223.

Tian, R.C., Hu, F.X., Martin, J.M., 1993. Summer nutrient fronts in the Changjiang (Yangtze River) estuary. Estuarine, Coastal and Shelf Science 37, 27-41.

Tomczak, M., 1981. A multi-parameter extension of temperature/salinity diagram techniques for the analysis of non-isopycnal mixing. Progress in Oceanography 10, 147-171.

Van Bennekom, A.J., Berger, G.W., Helder, W., De Vries, R.T.P., 1978. Nutrient distribution in the Zaire estuary and river plume. Netherlands Journal of Sea Research 12, 296-323.

Wang, H., Dai, M., Liu, J., Kao, S.J., Zhang, C., Cai, W.J., Wang, G., Qian, W., Zhao, M., Sun, Z., 2016. Eutrophication-Driven Hypoxia in the East China Sea off the Changjiang Estuary. Environmental Science & Technology 50, 2255-2263.

Weber, S.C., Carpenter, E.J., Coles, V.J., Yager, P.L., Goes, J., Montoya, J.P., 2017. Amazon river influence on nitrogen fixation and export production in the western tropical north Atlantic. Limnology and Oceanography 62, 618-631.

Wu, M.L., Hong, Y.G., Yin, J.P., Dong, J.D., Wang, Y.S., 2016. Evolution of the sink and source of dissolved inorganic nitrogen with salinity as a tracer during summer in the Pearl River Estuary. Scientific Reports 6, 36638.

Ye, F., Ni, Z., Xie, L., Wei, G., Jia, G., 2015. Isotopic evidence for the turnover of biological reactive nitrogen in the Pearl River Estuary, south China. Journal of Geophysical Research: Biogeosciences 120, 661–672.

Zhang, J., Liu, S.M., Ren, J.L., Wu, Y., Zhang, G.L., 2007. Nutrient gradients from the eutrophic Changjiang (Yangtze River) estuary to the oligotrophic Kuroshio waters and re-evaluation of budgets for the East China Sea shelf. Progress in Oceanography 74, 449-478.

List of Figures

Figure 1. Study sites and sampling area: (a) the sampling areas within the northern GOM including all LATEX and NEGOM stations (contour depth 200m); (b) shows only the region likely affected by MARS inputs (contours 10, 20, 50m). The different colors are the various projects (green, LATEX; orange, NEGOM; blue, LUMCON; red, MCH). The C line is near the Mississippi River (90°W to 89°W) and the F line is near the Atchafalaya River (~ 91°30’W). MCH data are widely distributed across the region; these station positions are from March 2005. We used only NEGOM data from the two lines nearest to the MR mouth at ~90° and 92°W.

Figure 2. DIN fluxes from the Atchafalaya River at Morgan City and the Mississippi River at Baton Rouge (data are from USGS). Data are monthly values of daily means from USGS (February 18, 2015 through October 22, 2016) to compare the two periods with consistent data sampling. (a) shows river discharges (m^3 s^{-1}), (b) concentration of NO_{3+2}, and (c) indicates nitrate + nitrite flux (mol day^{-1}). Baton Rouge has fewer data than Morgan City. In all graphs Atchafalaya River data are blue, Mississippi River data red.

Figure 3. Graphical concept for defining the edges of the three zones using nutrient/salinity changes, as modified from RC02. While production is still occurring in the blue zone, this is very low because of the low nutrients. The red dotted line indicates the theoretical mixing line and the blue shaded triangle indicates theoretical removal through biological uptake in the brown and green zones. Note that the concentrations on the salinity axis do not define the actual area of each zone, merely the relevant salinity range.

Figure 4. DIN and DSi data from above the pycnocline from the only winter MCH cruise (March 2005). Blue symbols are from stations close to the Atchafalaya, red from those close to the Mississippi. Brown, Green, and Blue dotted boxes were separated by plots of DIN and DSi concentration against salinity. Station positions are shown in Figure 1. PSS-78 is a salinity unit, Practical Salinity Scale 78.

Figure 5. As in Figure 4, but from the LATEX (February 1993) cruise. Blue symbols are from the line near 92°W, red from the line near 90°W.

Figure 6. Nutrient/salinity relationships for all LUMCON winter data (2001~2010) from above the pycnocline. Red dots are from the C line data and blue dots are from the F line. The black line shows the relationship given by the regression equation, bold green lines indicate estimated nutrient/salinity relationships based on river water end members and the dotted vertical line at S=33 is taken as the control for open water.

Figure 7. As in Fig. 6 for specific LUMCOM winter cruises (March 2001, 2003, 2009 and November 2004). Red dots are C line data and blue dots are F line data. These four cruises show similar patterns to MCH and LATEX data.

Figure 8. The three zones as determined using data from MCH cruises M1 to M5 and M8.

Figure 9. The three zones from the April (MCH M1), June (MCH M2), and August 2004 (MCH M3) cruises as determined by Lahiry (2007), based solely on salinity.

List of Tables

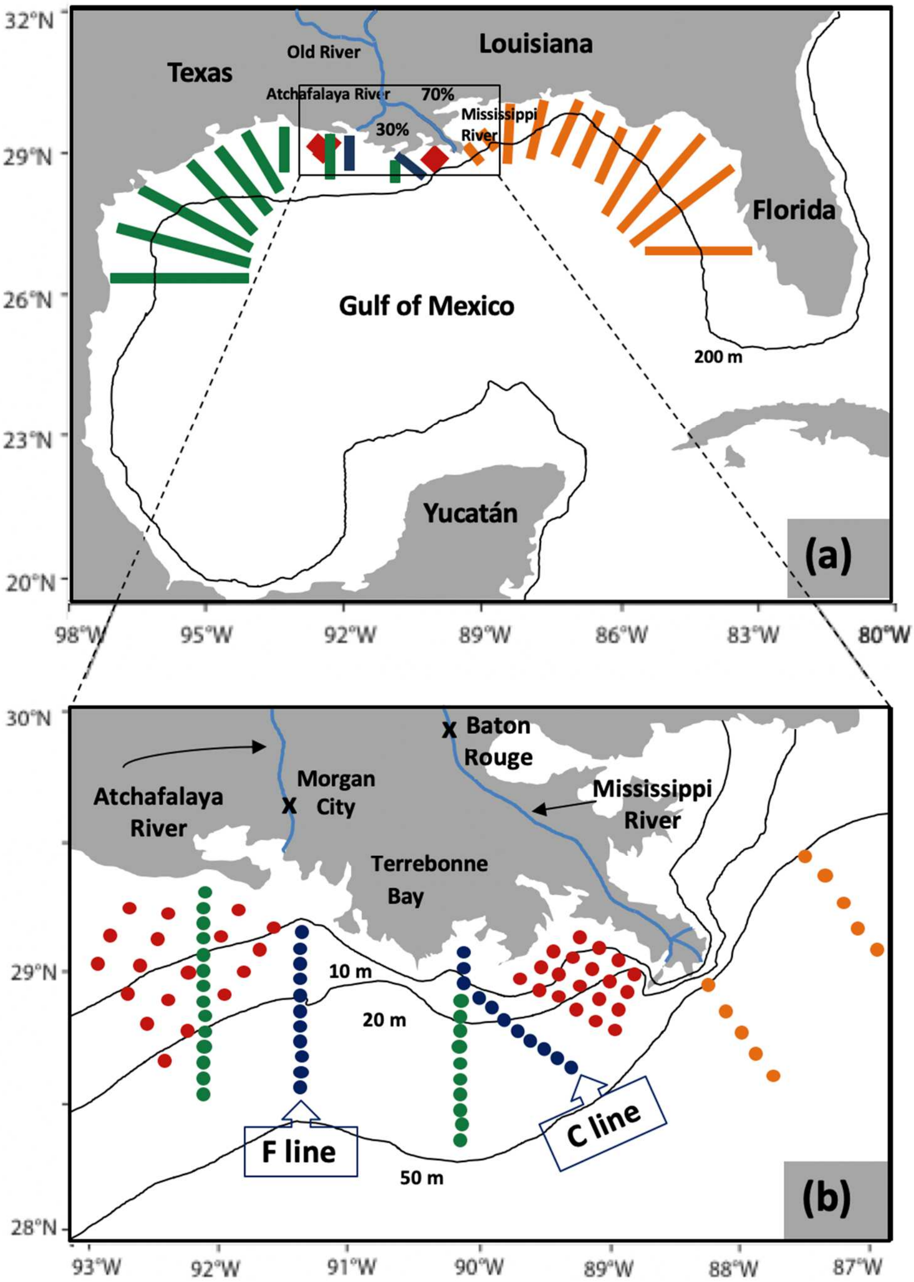

Figure 1. Study sites and sampling area: (a) the sampling areas within the northern GOM including all LATEX and NEGOM stations (contour depth 200m); (b) shows only the region likely affected by MARS inputs (contours 10, 20, 50m). The different colors are the various projects (green, LATEX; orange, NEGOM; blue, LUMCON; red, MCH). The C line is near the Mississippi River (90°W to 89°W) and the F line is near the Atchafalaya River (~ 91°30'W), respectively. MCH data are widely distributed across the region; these station positions are from March 2005. We used only NEGOM data from the two lines nearest to the MR mouth at ~90° and 92°W.

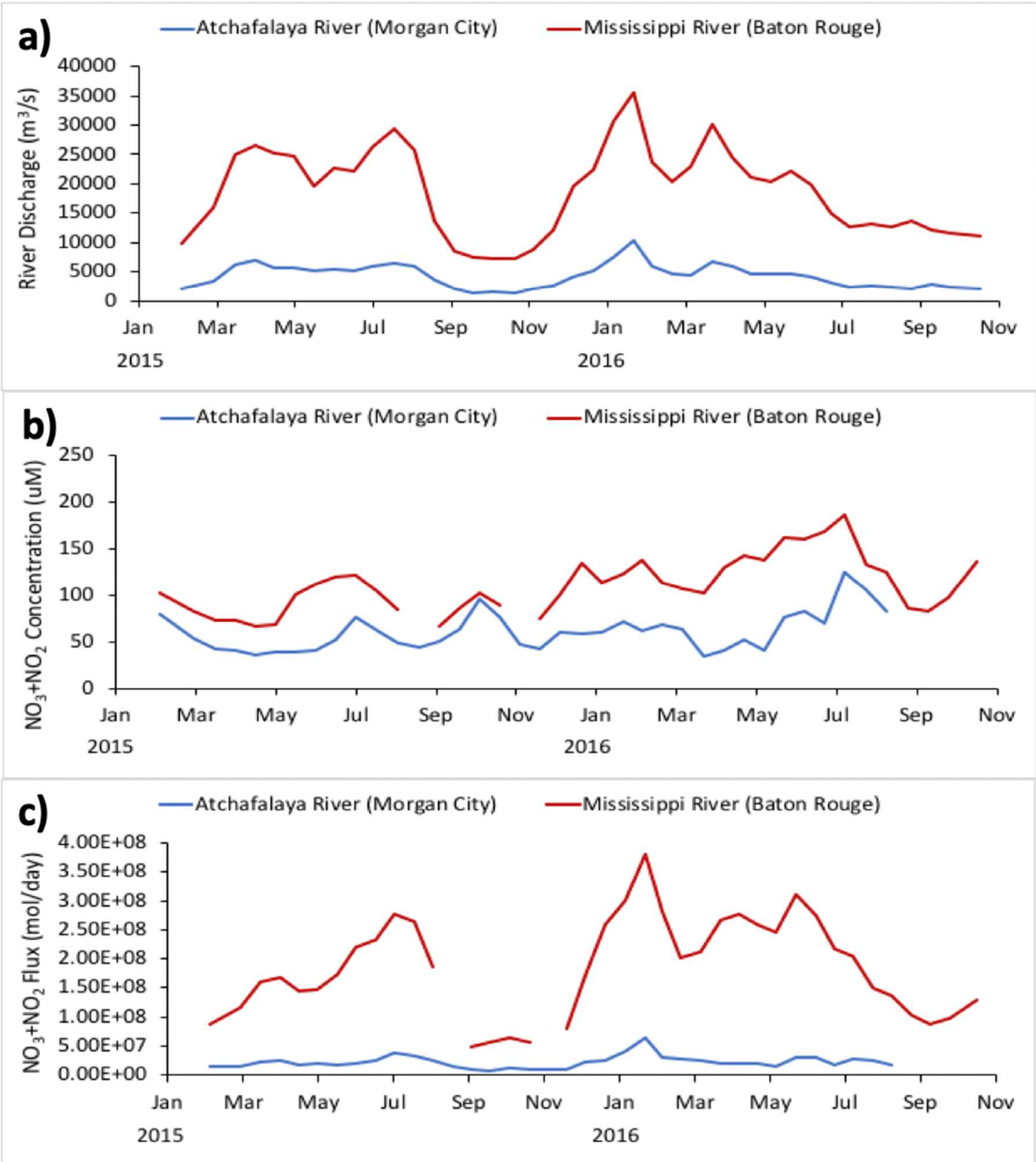

Figure 2. DIN fluxes from the Atchafalaya River at Morgan City and the Mississippi River at Baton Rouge (data are from USGS). Data are monthly values of daily means from USGS (February 18, 2015 through October 22, 2016) to compare the two periods with consistent data sampling. (a) shows river discharges (m^3 s^{-1}), (b) concentration of NO_{3+2}, and (c) indicates nitrate + nitrite flux (mol day^{-1}). Baton Rouge has fewer data than Morgan City. In all graphs Atchafalaya River data are blue, Mississippi River data red.

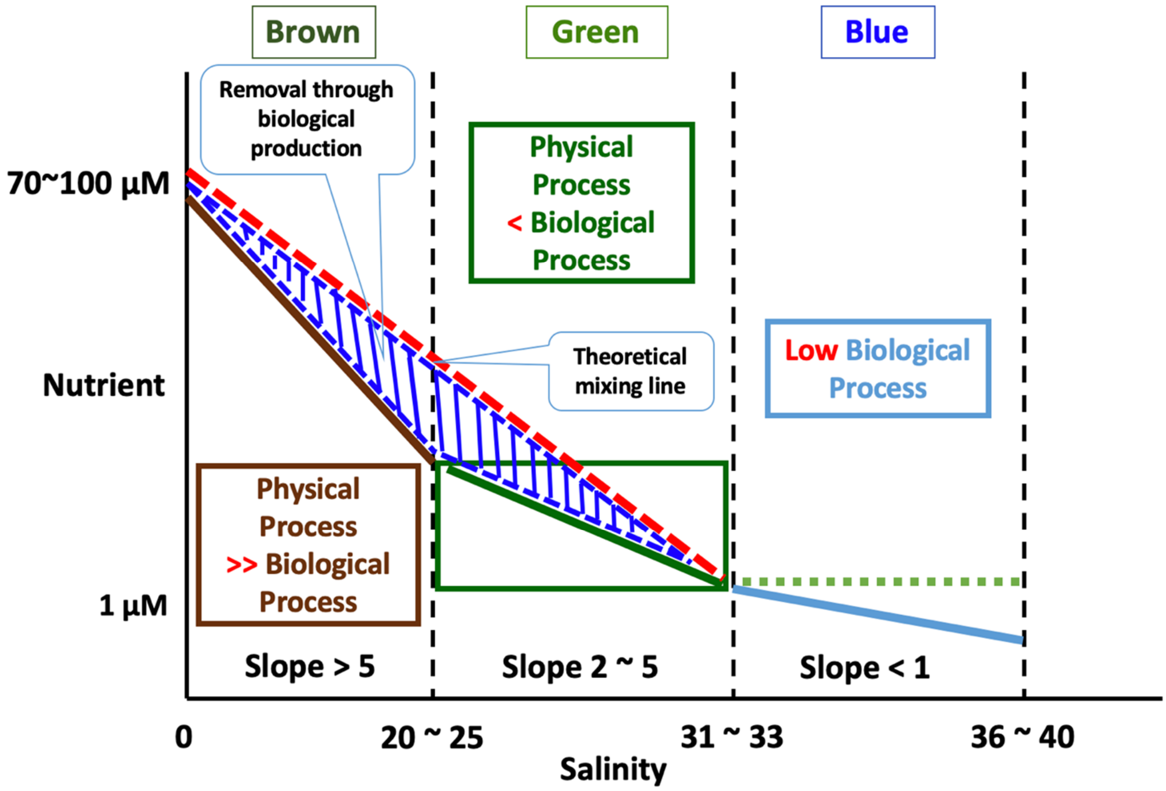

Figure 3. Graphical concept for defining the edges of the three zones using nutrient/salinity changes, as modified from RC02. While production is still occurring in the blue zone, this is very low because of the low nutrients. The red dotted line indicates the theoretical mixing line and the blue shaded triangle indicates theoretical removal through biological uptake in the brown and green zones. Note that the concentrations on the salinity axis do not define the actual area of each zone, merely the relevant salinity range.

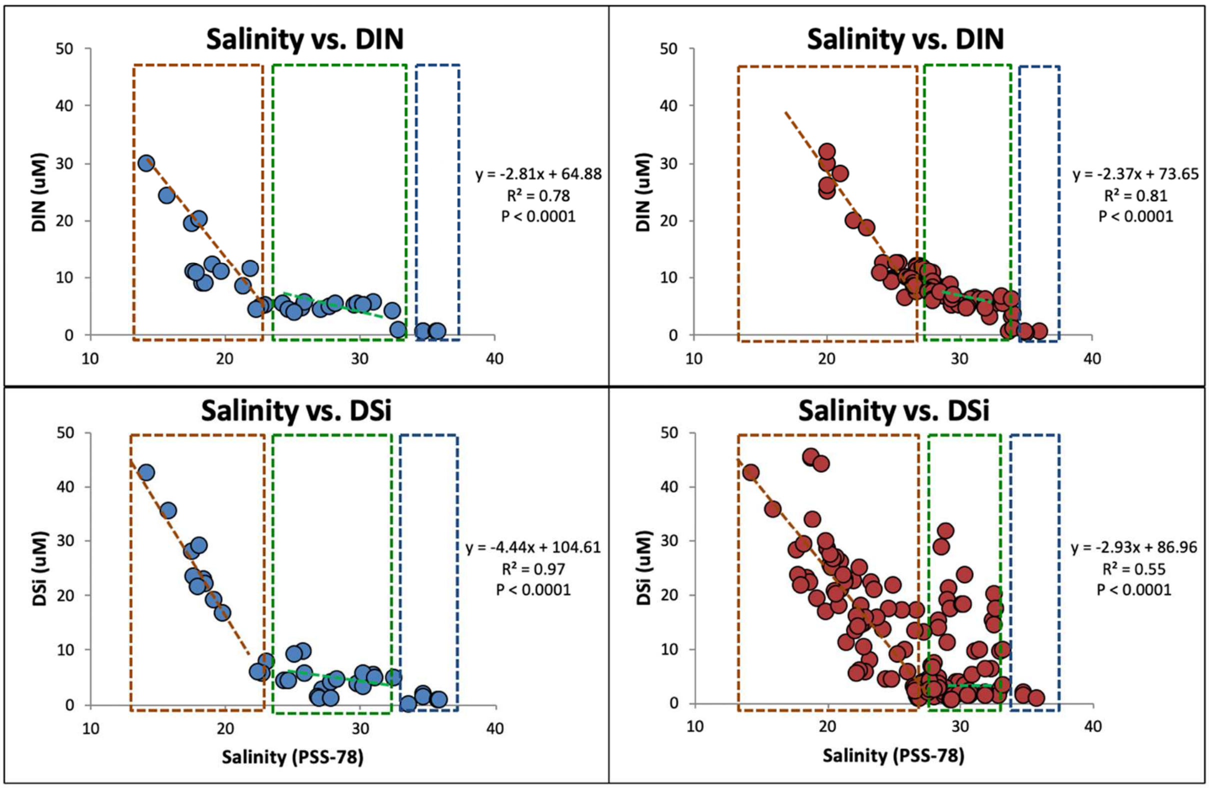

Figure 4. DIN and DSi data from above the pycnocline from the only MCH winter cruise (March 2005). Blue symbols are from stations close to the Atchafalaya, red from those close to the Mississippi. Brown, Green, and Blue dotted boxes were separated by plots of DIN and DSi concentration against salinity. Station positions are shown in Figure 1. PSS-78 is a salinity unit, Practical Salinity Scale 78.

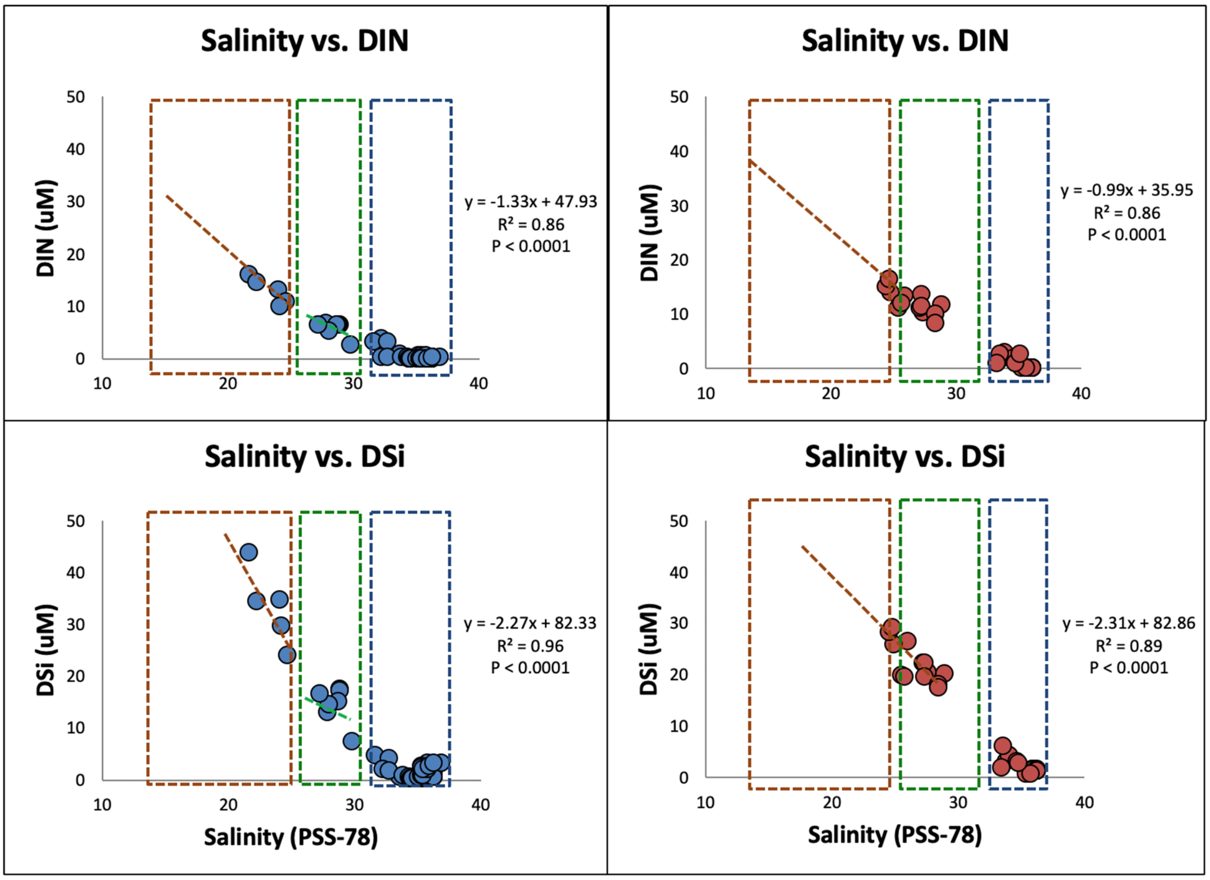

Figure 5. As in Figure 4, but from the LATEX (February 1993) cruise. Blue symbols are from the line near 92°W, red from the line near 90°W.

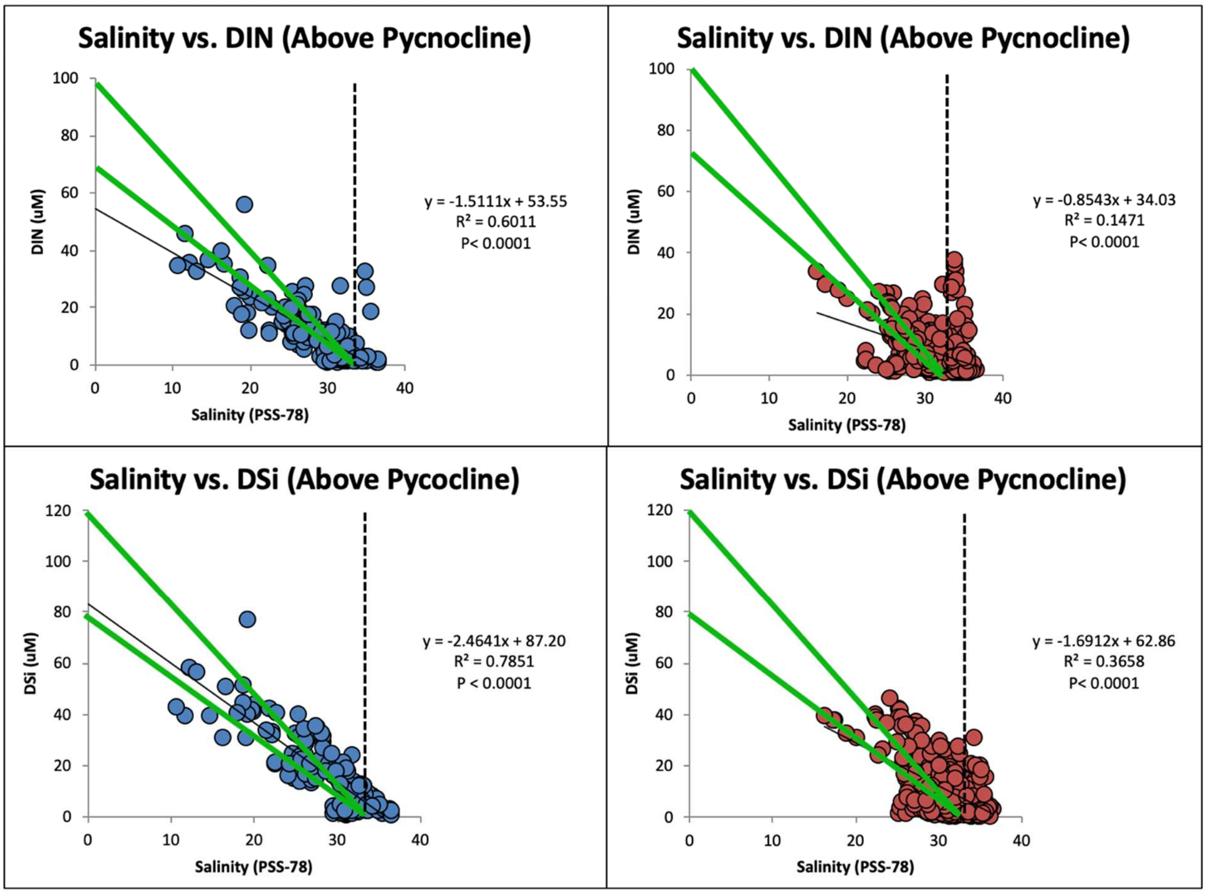

Figure 6. Nutrient/salinity relationships for all LUMCON winter data (2001~2010) from above the pycnocline. Red dots are from the C line data and blue dots are from the F line data. The black line shows the relationship given by the regression equation, bold green lines indicate estimated nutrient/salinity relationships based on river water end members and the dotted vertical line at S=33 is taken as the control for open water.

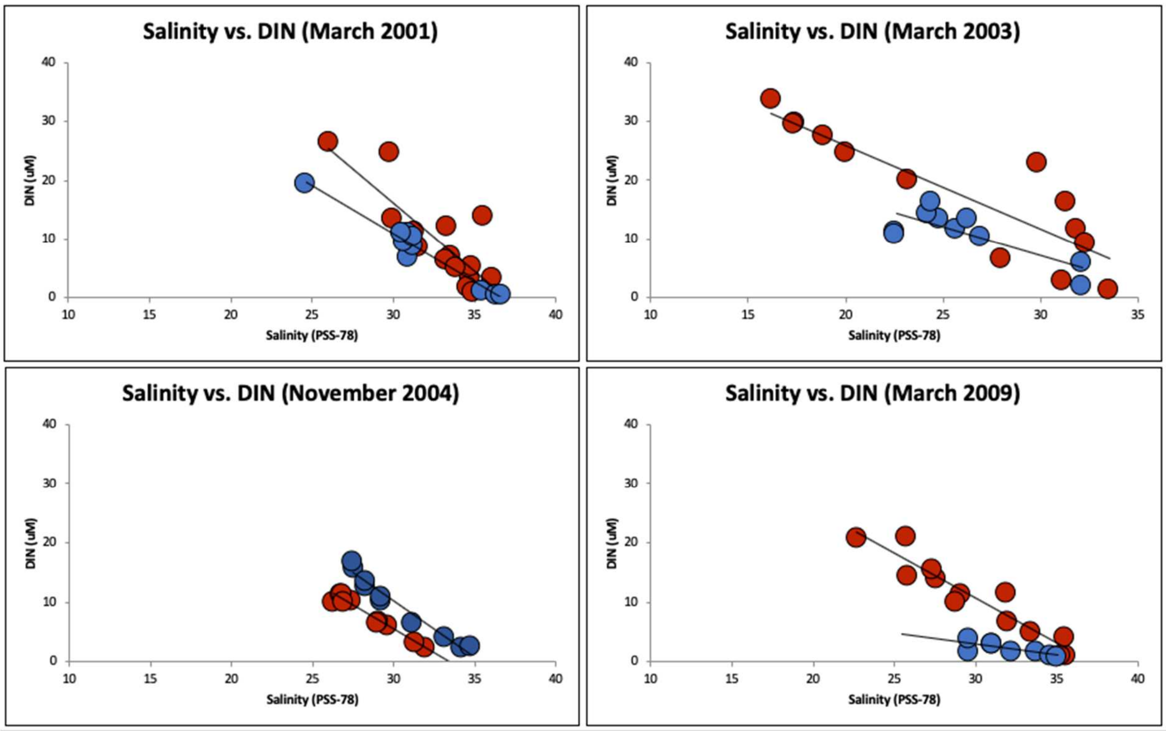

Figure 7. As in Fig. 6a for specific LUMCOM winter cruises (March 2001, 2003, 2009 and November 2004). Red dots are C line data and blue dots are F line data. These four cruises show similar patterns to MCH and LATEX data.

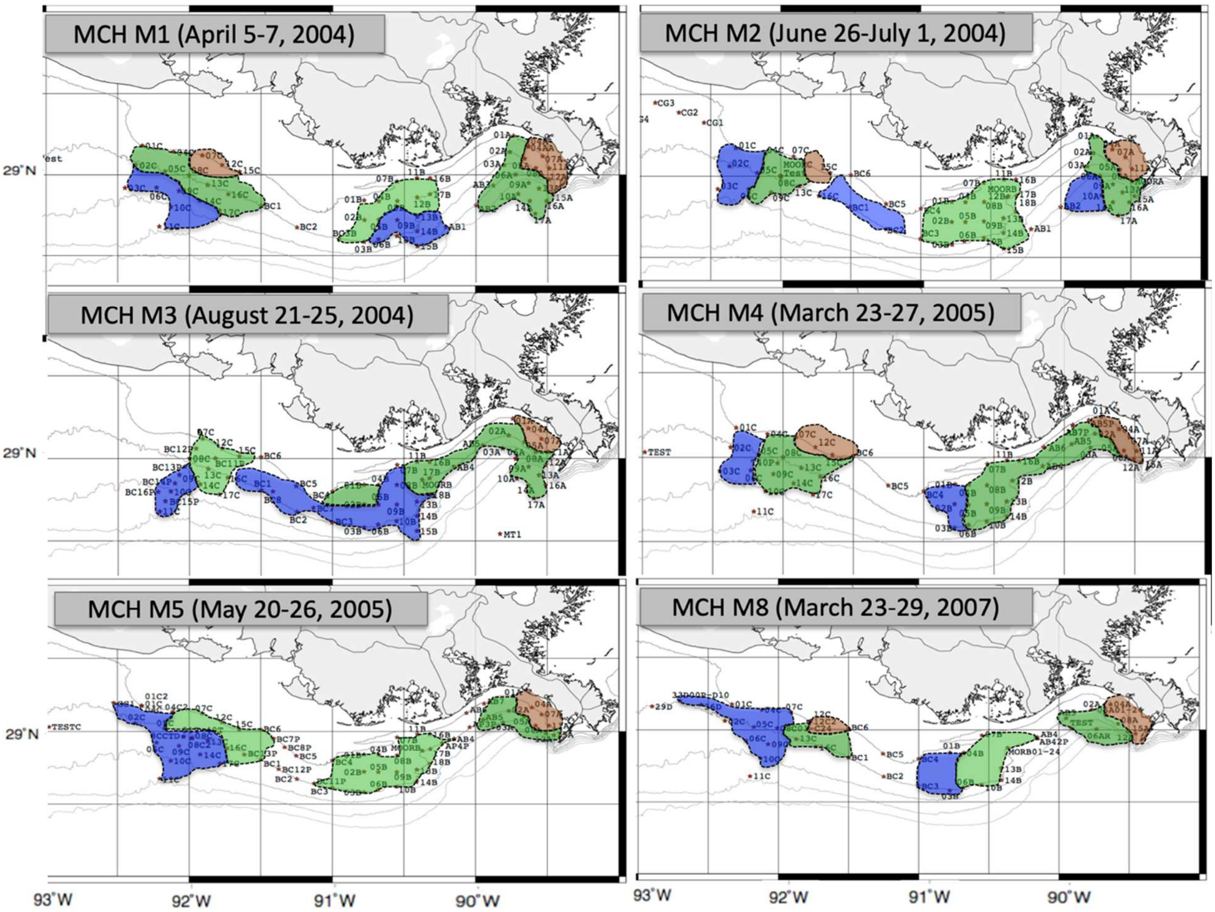

Figure 8. The three zones as determined using data from MCH cruises M1-M5 and M8.

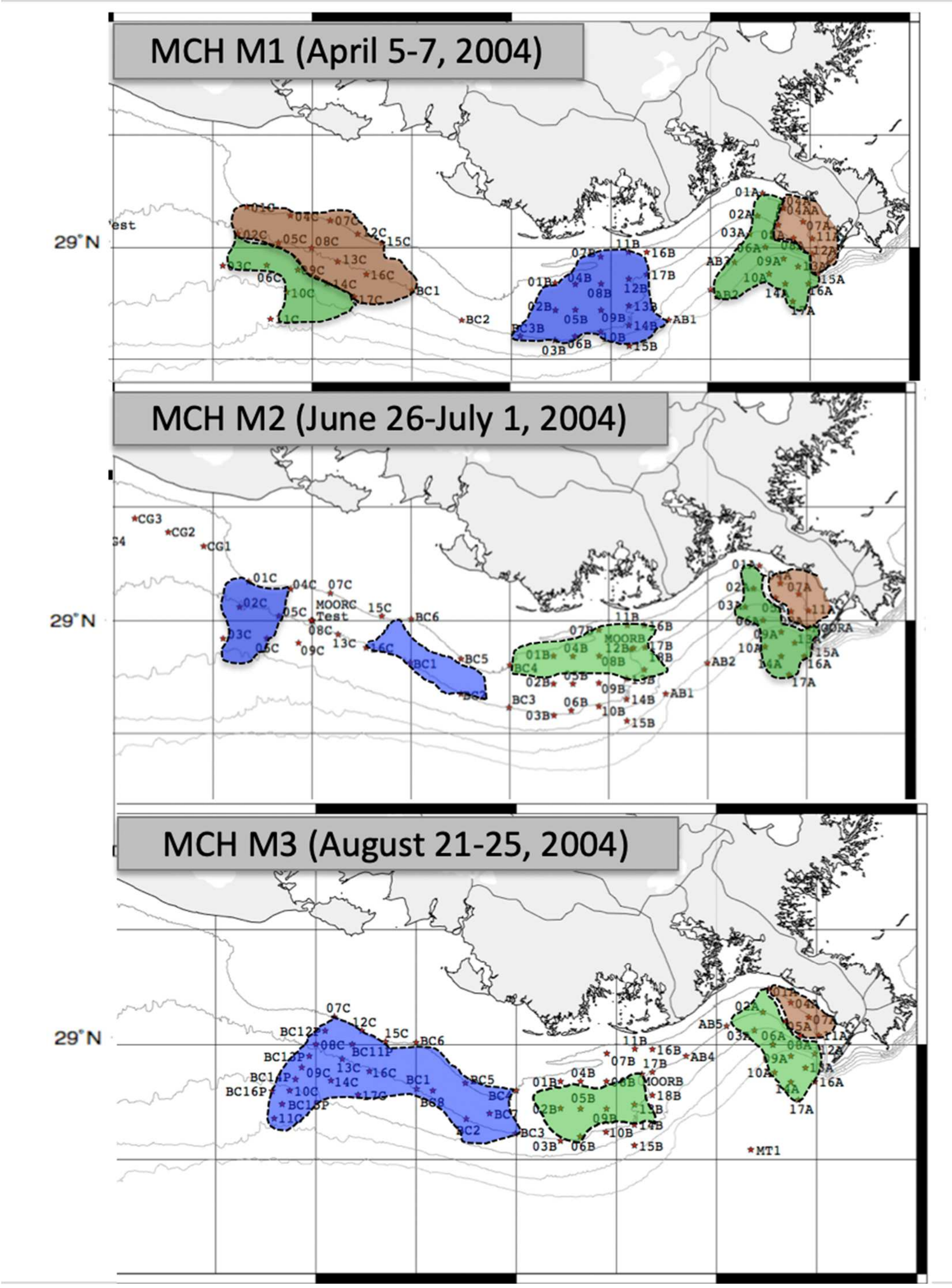

Figure 9. The three zones from the April (MCH M1), June (MCH M2), and August 2004 (MCH M3) cruises as determined by Lahiry (2007), based solely on salinity.

Table 1. Sampling dates for data from Gulf of Mexico projects.

Project	Non-winter data	Winter data
LATEX	May, Aug, Nov- 1992 May, Aug, Nov- 1993 May, Aug, Nov- 1994	Feb-1993
LUMCON	1998~2010 (Monthly)	Jan, Feb, Mar, Nov, Dec (2001-2010)
MCH	April 5~7, 2004 June 26~July 1, 2004 August 21~25, 2004 May 20~26, 2005 March 23~29, 2007	March 23~27, 2005
NEGOM	May 13~16, 1998 August 4~6, 1998 May 25~27, 1999 August 18~20, 1999 April 23~26, 2000 July 29~30, 2000	November 24~26, 1997 November 22~24, 1998 November 13~15, 1999

Table 2. Freshwater end-member range, median, standard deviation, and average from DIN concentration at Morgan City and Baton Rouge, respectively, for data shown in Figure 2 and for USGS monthly data from 2000-2018.

	DIN	Morgan City	Baton Rouge
Daily data 2015-2016	**Freshwater range (Annual)**	70 ~ 100 μM	70 ~ 100 μM
	Average	74.05 μM	87.4 μM
	Median	69.97 μM	81.02 μM
	Std. Dev.	22.51 μM	35.01 μM
Monthly data 2000-2018	**Range**	30 ~ 190 μM	20 ~ 220 μM
	Average	79.29 μM	99.97 μM
	Median	74.26 μM	98.53 μM
	Std. Dev.	33.61 μM	42.81 μM

Table 3. DIN/salinity relationships for LUMCON winter data, showing correlation coefficient, predicted end-member, and nutrient/salinity slopes. X signifies salinity, y the estimated DIN concentration in µM/L.

LUMCON monthly cruises	**Near Mississippi River (C)**	**Near Atchafalaya River (F)**
January, 2001	y = -2.3036x + 107.33 R^2 = 0.1399	y = -0.4858x + 41.88 R^2 = 0.2237
March, 2001	y = -2.334x + 86.269 R^2 = 0.6757	y = -1.6381x + 60.107 R^2 = 0.9604
November, 2001	y = -1.2254x + 43.976 R^2 = 0.9292	y = -1.7561x + 59.9 R^2 = 0.8754
February, 2002	y = -1.3522x + 51.01 R^2 = 0.8764	y = -1.3401x + 48.73 R^2 = 0.9283
December, 2002	y = -0.7131x + 27.325 R^2 = 0.4	y = -2.1573x + 70.784 R^2 = 0.9598
January, 2003	y = 0.1063x + 3.5358 R^2 = 0.003	y = -1.3455x + 44.394 R^2 = 0.8901
March, 2003	y = -1.4346x + 54.667 R^2 = 0.7727	y = -0.9788x + 36.528 R^2 = 0.6314
December, 2003	y = 0.0429x - 0.7279 R^2 = 0.0098	y = -1.9681x + 61.758 R^2 = 0.9054
February, 2004	y = -1.1443x + 47.929 R^2 = 0.4429	y = -1.7824x + 68.104 R^2 = 0.9869
November, 2004	y = -1.604x + 53.652 R^2 = 0.9638	y = -1.8935x + 67.126 R^2 = 0.9568
March, 2007	y = -0.163x + 9.1491 R^2 = 0.0302	y = -0.0437x + 2.3387 R^2 = 0.4381
January, 2009	y = -1.4346x + 54.667 R^2 = 0.7727	y = -0.9788x + 36.528 R^2 = 0.6314
March, 2009	y = -1.5176x + 56.178 R^2 = 0.9078	y = -0.3627x + 13.792 R^2 = 0.5809
March, 2010	y = 0.1046x + 1.6485 R^2 = 0.0809	y = 0.3029x - 4.4944 R^2 = 0.0069

Table 4. Salinities for brown-green and green-blue zone boundaries in various large rivers. Where no value is given for the brown/green boundary, mixing was conservative throughout the region affected. Separate salinities for the breaks in the nutrient/salinity plots are given for nitrate and silicate where indicated.

River	Date	Brown-Green	Green-Blue	Reference
Amazon	Aug, 1989	18-20	34-36	
	Mar, 1990	10	12 (N), 25 (Si)	DeMaster and Pope (1996)
	May, 1990	10	12 (N), 35 (Si)	
	Nov, 1991	13-15	15 (N), 20 (Si)	
	May, 2010	< 16.6 (N), 18 (Si)	< 16.6 (N), 33-34 (Si)	Weber et al. (2017)
Atchafalaya	Feb, 1993	30	33	This study
	Mar, 2005	22	33	
	Various	< 25	> 32	LUMCON
Changjiang	June, 1980	18 (N), 20 (Si)	> 30	Edmond et al. (1985)
	Nov, 1981	-	> 32	
	1985-1986	4-6	30	Shen (1993)
	Aug, 1988	25	26 (Si), 28 (N)	Tian et al. (1993)
	July, 2001	-	> 30	Zhang et al. (2007)
	Aug, 2002	20	24	
	2011-2012	20 (Summer)	25-27	Gao et al. (2015)
	2011-2012	- (Winter)	35	
	Aug, 2002	16	> 28	Liu et al. (2016)
Mississippi	Feb, 1993	31-32	33	This study
	Mar, 2005	28	33	
	Various	< 25	> 33	LUMCON
Para	Nov, 1991	5 (N), 10 (Si)	30	DeMaster and Pope (1996)
Zaire	Nov, 1976	25-27	32 (N)	Van Bennekom et al. (1998)
	May, 1978	25-27	30 (N)	